PCCP

Cite this: *Phys. Chem. Chem. Phys.*, 2012, **14**, 8945–8955

www.rsc.org/pccp

PAPER

H-bonded network rearrangements in the S_0, S_1 and D_0 states of neutral and cationic *p*-cresol(H_2O)(NH_3) complexes†

Federico J. Hernández,[a] Marcela C. Capello,[a] Andrés N. Oldani,[a] Juan C. Ferrero,[a] Philippe Maitre[b] and Gustavo A. Pino*[a]

Received 14th November 2011, Accepted 16th January 2012
DOI: 10.1039/c2cp23586b

The H-bonded network rearrangements in the S_0, S_1 and D_0 states of the neutral and cationic *p*-CreOH(H_2O)(NH_3) complexes were studied experimentally by means of (1 + 1)/(1 + 1′) REMPI (Resonantly Enhanced MultiPhoton Ionization) and time resolved LIF (Laser Induced Fluorescence) spectroscopies combined with DFT (Density Functional Theory) calculations at the B3LYP/6-311G++(d,p) level. A comparison of the rearrangement process of the H-bonded network in the three states is given. Two cyclic H-bonded isomers were found on the S_0 potential energy surface and the results indicate that the rearrangement in this state is unlikely at the temperature of the supersonic expansion due to the presence of a high-energy barrier (7503 cm^{-1}). On the other hand, the re-determination of the S_1 excited state lifetimes confirms that neither the H-bonded rearrangement nor the excited state hydrogen transfer (ESHT) reaction takes place in the S_1 state at the excitation energies of this work. Thus, it is concluded that the absorption of the second photon to reach the D_0 state takes place from the S_1 state of the cyclic-(OH–OH_2–NH_3) isomer. A preferential evaporation of H_2O upon vertical ionization of the cyclic-(OH–OH_2–NH_3) isomer is observed which is consistent with a statistical redistribution of the internal energy. Nevertheless, our theoretical calculations suggest that initial excitation of the H-bonded network rearrangement modes may also play a role to leave the H_2O molecule as a terminal moiety in a chain-$(OH–NH_3–OH_2)^+$ isomer. The reaction pathway for the solvent rearrangement involves a double proton transfer process with a very low energy barrier (575 cm^{-1}) that is overcome at the vertical ionization energy of the complex.

1. Introduction

Hydrogen-bonding is a contemporary research interest because of its fundamental importance in many branches of science.[1] Hydrogen-bonding interactions play an important role in stabilizing the structure, which in turn controls the function, of macromolecular systems such as proteins.[2,3] The strong solvating capacity of water is also due in large part to the formation of H-bonds with hydrophilic solute. The full solvation shell is a complex network of many H-bonded water molecules. The physical and reactive properties of the embedded solute are the result of a subtle interplay between solvent–solvent and solute–solvent interactions, which are difficult to separate.

Solvent–solute clusters in the gas-phase constitute simple model systems of complex H-bonded networks in the condensed phase. Sophisticated laser spectroscopic techniques combined with supersonic expansion have been extensively used to study H-bonded clusters at the molecular level. In addition, these experimental studies can be easily coupled with quantum chemical calculations, and many reports on the structures of H-bonded clusters and the static characters of the H-bonds have been published.[4–8]

One interesting facet of the H-bonds properties is the fluctuation or rearrangement of H-bonded networks that are associated with structural changes of solute biomolecules. Several studies of these fluctuations in neutral and cationic H-bonded complexes in the gas phase have been reported.[1,9–14] Upon photoexcitation of hydrogen-bonded systems, the hydrogen donor and acceptor molecules reorganize due to the significant difference in the charge distribution of different electronic states, which induces the excited state hydrogen bonding dynamics.[1] For example, the dynamics of the photoinduced solvent rearrangement in the S_1 state of the 7-azaindole(H_2O)$_3$ complex has been recently investigated.[9] Upon excitation to the S_1 state, solvent isomerization from a chain-like to a cycle-like isomer was characterized at the picosecond timescale using Resonantly Enhanced MultiPhoton Ionization (REMPI) spectroscopy.[9] Many other examples on the excited state hydrogen bonding dynamics are given in a very recent review.[1] The migration of a single water

[a] *INFIQC, Dpto. de Fisicoquímica, Fac. de Ciencias Químicas, Centro Láser de Ciencias Moleculares, Universidad Nacional de Córdoba, Ciudad Universitaria, Pabellón Argentina, 5000 Córdoba, Argentina. E-mail: gpino@fcq.unc.edu.ar*
[b] *Laboratoire de Chimie Physique, Faculté des Sciences, Université Paris Sud, UMR8000 CNRS, Bât. 350-91405, Orsay Cedex, France*
† Electronic supplementary information (ESI) available. See DOI: 10.1039/c2cp23586b

molecule between the NH group and the CO group on *trans*-formanilide in the S_0 state of the *trans*-formanilide(H_2O) complex was induced by stimulated emission pumping population transfer spectroscopy.[10] The same effect was observed in the D_0 state of the [*trans*-acetanilide(H_2O)]$^+$ cation by IR-dip spectroscopy.[11] The migration of a water molecule from a CO group to a NH_2 group was also observed in the biologically relevant [phenylglycine(H_2O)]$^+$ cation, analysing the REMPI spectra measured on the channel masses of different photofragments.[12] A similar water migration from the OH group to the NH_2 group was also reported to occur in the D_0 state of the [4-aminophenol(H_2O)]$^+$ cation, studied by means of mass analyzed threshold ionization (MATI) and IR-UV double resonance spectroscopy.[13]

All these photoinduced solvent reorganizations involve the transfer of the water molecule between different functional groups within the same chromophore. However, the dynamics of photoinduced reorganization of solvent around a solute with a single H-bond donor and acceptor functional group has received less attention. There is only one very recent report on [*trans*-formanilide(H_2O)$_4$]$^+$ for which it was concluded that the driving force for the reorganization is entropic, due to the fact that the most populated isomer in the D_0 state is not the most stable one.[14]

The goal of this work was to provide more information on the H-bonded network structural fluctuations or rearrangements in the ground and excited states of neutral and cationic clusters in the gas phase with a different approach. Let us consider a chromophore with only one functional group, such as an aromatic alcohol (R–OH). It has the possibility to act simultaneously as both H-donor (R–OH$\cdots$XH) and H-acceptor (R–(H)O$\cdots$HX), where HX is a solvent molecule (X = NH_2 or OH). Then, a H-bonded cluster with two solvent molecules ($ROH(HX)_2$) could have a chain-like structure (R–OH$\cdots$X–H$\cdots$X–H/R–(H)O$\cdots$H–X$\cdots$H–X) or a cyclic-like structure (R-OH…X-H…X-H). Upon excitation, the H-bonded network could be rearranged and interconversion between the different structures could take place. With two different solvent molecules, the number of possible network structures and then interconversion possibilities are even higher.

In this context, the *p*-CreOH(H_2O)(NH_3) complex (*p*-CreOH = *p*-cresol) constitutes an interesting model system. First, two cyclic isomers (Fig. 1) were found on its S_0 ground state potential energy surface (PES).[15] One, hereafter denoted cyclic-(OH–OH_2–NH_3) (Fig. 1a), has the OH group of the chromophore acting as an H-bond donor to the H_2O molecule and as an H-bond acceptor from the NH_3 molecule. The other, hereafter denoted cyclic-(OH–NH_3–OH_2) (Fig. 1b), is only slightly higher in energy (ΔE = 238 cm^{-1} or 143 cm^{-1} including the zero point vibrational energy at the B3LYP/6-311G++(d,p) level). It has the chromophore OH group acting as an H-bond donor to the NH_3 molecule and as an H-bond acceptor from the H_2O molecule. By comparison of the REMPI and Laser Induced Fluorescence (LIF) spectra and the estimation of the excited state lifetime, it was concluded that the spectral features observed in the range 34 780–34 880 cm^{-1} correspond to the excitation of the lowest energy cyclic-(OH–OH_2–NH_3) structure.[15] Based on the small energy difference between the two cyclic structures, both isomers should have been present in the molecular beam. However, it was suggested that the non-observation of one of the isomers could be a result of absorption in a different spectral region or a too short excited state lifetime to be detected with nanosecond lasers.[15]

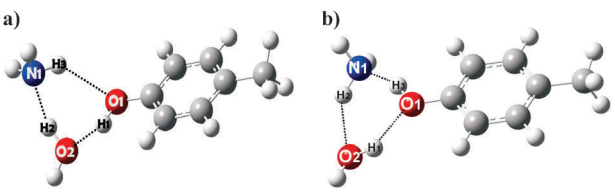

Fig. 1 Electronic ground state optimized structures of (a) cyclic-(OH–OH_2–NH_3) and (b) cyclic-(OH–NH_3–OH_2) isomers of the *p*-CreOH(H_2O)(NH_3) complex, obtained at the DFT-B3LYP/6-311G++(d,p) level of theory.

It was also reported that the excess energy deposited in the D_0 state of the ion *via* the $S_1 \leftarrow S_0$ transition of the cyclic-(OH–OH_2–NH_3) isomer is mostly dissipated by evaporation of H_2O.[15] An interesting question is then whether the selective loss of one of the solvent molecules is essentially driven by static phenomena, *i.e.* the initial structure of the H-bonded network in the S_0 state, or by the dynamics within the intermediate S_1 or the final D_0 state.

We herein present a comparison of the dynamics of H-bonded network rearrangements of the *p*-CreOH(H_2O)(NH_3) complex in the S_0, S_1 and D_0 states and propose an interpretation for the observed selective H_2O evaporation upon photoionization of cyclic-(OH–OH_2–NH_3), at all of the excitation energies studied. Experimental data have been complemented by density functional theory (DFT) calculations of the ionization energies and evaporation processes and characterization of the ground state potential energy surfaces of both neutral and ionic *p*-CreOH(H_2O)(NH_3) clusters.

While in the S_0 and S_1 states, the H-bonded network rearrangement does not take place at the applied excitation energy, the results suggest that the observed preferential water loss in the D_0 state is driven by the dynamics associated with a complex structural rearrangement of the vibrationally excited *p*-CreOH(H_2O)(NH_3)$^+$ cluster. This energetically most favourable channel can be reached after a solvent rearrangement assisted by a double proton transfer in the D_0 state of the cation. As compared to a direct NH_3 loss, *i.e.* a simple bond cleavage, this process is likely to be entropically disfavoured since it proceeds through a tight transition state. Although the results indicate that a statistical behaviour can explain the preferential H_2O loss, the analysis of differential geometry between the vertical and adiabatic geometries of the ionic cluster suggests that the dynamics of H-bonded network rearrangement, that precedes that H_2O evaporation, is favoured by the excited vibrational state of the initially formed ionic cluster.

2. Experimental and theoretical methods

The apparatus used for resonantly enhanced multiphoton ionization (REMPI) was described elsewhere.[15,16] Briefly, the clusters were generated in two differentially pumped chambers, by expanding a mixture of He seeded with NH_3 (0.5%) that passed over a reservoir containing *p*-CreOH heated to 40–70 °C to increase its vapour pressure. The stagnation pressure was typically 1–3 bar and it was expanded to vacuum through

a 400 μm diameter pulsed nozzle (Solenoid General Valve, Serie 9). Because of the strong hygroscopic property of *p*-CreOH, the water present in the sample was high enough for these experiments. However, some experiments were performed with controlled added water and very large water containing clusters were produced under these conditions which lead to a broad continuum background in the excitation spectra that masked the structured spectra of the smaller complexes.

The skimmed molecular beam was crossed by the laser beams at right angle in the ionization chamber. The ions were extracted in a home-built Wiley–McLaren type time-of-flight (TOF) mass spectrometer (46 cm flight length), perpendicular to the molecular beam and laser directions, and entered the drift chamber, where they were detected using a multichannel plate (Del Mar Ventures MCP-MA34).

For the Time Resolved Laser Induced Fluorescence (TR-LIF) experiments the jet was intercepted, at right angle, by the laser beam at 1.5 cm from the nozzle. The fluorescence was collected by a telescope collinear to the jet and detected by a photomultiplier tube (PMT) (Hammamatsu R636) without any filter.

The TR-LIF experiments and REMPI spectra were performed using a frequency doubled Lumonics (HD500) dye laser (FWHM = 5 ns) operating with a mixture of Rhodamine 590 and 610, pumped by the second harmonic of a Spectra-Physics (Indi-HG) Nd:YAG laser. The same laser system was used to pump the complexes to the first singlet excited state (S_1) in the two colour experiments performed to determine the ionization potentials (IPs) and evaporation thresholds of the complexes. The ionization source was a frequency doubled Spectra-Physics (Sirah, Cobra-Strech) dye laser (FWHM = 5 ns) operating with Pyridine 1 360–330 nm, DCM 330–309 nm and a mixture of Rhodamine 610 and 640 315–304 nm and pumped by the second harmonic of a Quantel (Brillant-B) Nd:YAG laser.

The signals from the PMT and the MCP were averaged and digitized by a Tektronik (TDS-3034B) oscilloscope and integrated with a PC. The rise time of the complete detection system was below 1 ns.

Quantum chemical calculations were carried out with the GAUSSIAN 03 program package[17] using the B3LYP hybrid density functional. Kohn–Sham orbitals were expended in the 6-311G++(d,p) basis set and the unrestricted approach was used for the open shell systems.

3. Results

3.a Experimental results

3.a.(i) REMPI spectra and S_1 state lifetime re-determination. Fig. 2a–c show the REMPI (1 + 1) spectra, recorded on the masses of the parent *p*-CreOH$(H_2O)(NH_3)^+$ ion complex and the daughter *p*-CreOH$(NH_3)^+$ and *p*-CreOH$(H_2O)^+$ ions, respectively. In previous studies,[15] the vibronic band at 34 792 cm^{-1} which is red-shifted by 539 cm^{-1} from the 0_0^0 transition of bare *p*-CreOH was assigned to the $S_1 \leftarrow S_0$ origin band of the cyclic-(OH–OH_2–NH_3) isomer of the mixed *p*-CreOH$(H_2O)(NH_3)$ complex while the band at 34 873 cm^{-1} observed in Fig. 2b was assigned to the intermolecular stretching (σ_0^1) of the *p*-CreOH(NH_3) complex.[16] Spectra (a) and (b) have been previously reported, however it is the first time that

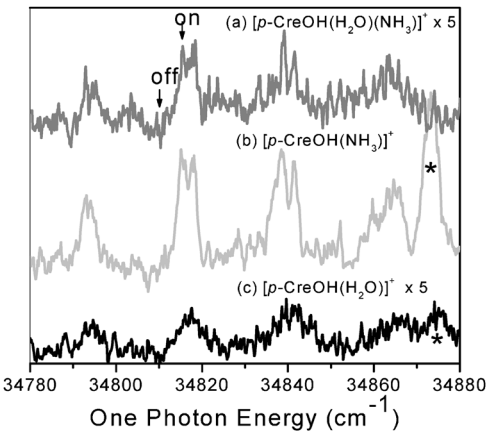

Fig. 2 Mass resolved (1 + 1) REMPI spectra recorded at the masses of (a) [*p*-CreOH$(H_2O)(NH_3)]^+$ (——), (b) [*p*-CreOH$(NH_3)]^+$ (——) and (c) [*p*-CreOH$(H_2O)]^+$ (——). The intensities of spectra (a) and (c) are multiplied 5×. The labels *on* and *off* indicate the excitation energies *on* and *off* resonance, respectively, used to determine the ionization and evaporation threshold shown in Fig. 3.

the spectral signature of the parent complex is observed on the *p*-CreOH$(H_2O)^+$ ions mass (spectrum (c)), indicating that although a minor channel, NH_3 evaporation also takes place upon one-colour two-photon ionization.

The excited state lifetime of the cyclic-(OH–OH_2–NH_3) isomer was determined previously by TR-LIF to be 12 ± 2 ns,[15] while that of the *p*-CreOH(H_2O) was 15 ± 2 ns,[15] which was larger than the value 3.8 ± 0.5[18] ns obtained from the linewidth of a rotational line. This disagreement leads us to re-determine the excited state lifetimes of both complexes with a shorter rise-time detection system upon excitation to several transitions. The excited state lifetime of the cyclic-(OH–OH_2–NH_3) complex was determined by exciting each of the four transitions shown in Fig. 2 within 75 cm^{-1} above the origin of the electronic transition and those of the *p*-CreOH(H_2O) complex upon excitation to the $S_1 \leftarrow S_0$ origin as well as to the σ^1 vibronic level corresponding to the intermolecular stretching mode. Table 1 shows the excited state lifetimes of both complexes determined at different internal energies in the S_1 state together with the corresponding values for the *p*-CreOH(NH_3) complex reported in the literature.[19] It is observed that the S_1 lifetime for the water containing complexes is independent of the vibrational excitation at variance with the S_1 lifetime of the *p*-CreOH(NH_3) complex.[16,19]

The re-determined $S_1(0^0)$ state lifetime 3.8 ± 0.1 ns of the *p*-CreOH(H_2O) complex agrees better with the value τ = 3.8 ± 0.5[18] ns derived from the linewidth of a rotational line, than the previously TR-LIF determination.[15] As can be seen in Table 1, the behavior of the S_1 lifetime of *p*-CreOH$(H_2O)(NH_3)$ as a function of the internal energy is very similar to that of the *p*-CreOH(H_2O) complex, whereas it strongly differs from that of the *p*-CreOH(NH_3) complex. This leads us to re-confirm that only the cyclic-OH–OH_2–NH_3 isomer is at play under the present experimental conditions.

3.a.(ii) Ionization and evaporation thresholds determination. Fig. 2 shows the abundance of the parent *p*-CreOH$(H_2O)(NH_3)^+$ ion complex and the daughter *p*-CreOH$(NH_3)^+$ and

Table 1 Excited state (S_1) lifetimes determined by time resolved fluorescence of the *p*-CreOH(H_2O) and *p*-CreOH(H_2O)(NH_3) complexes upon laser excitation of different transitions. For comparison, the excited state lifetime of the 0^0 and σ^1 states of the *p*-CreOH(NH_3) complex, previously reported is also given

Excess energy/ cm^{-1}	*p*-CreOH(NH_3) τ/ns	*p*-CreOH(H_2O) τ/ns	Cyclic-(OH–$OH_2$$NH_3$) τ/ns
0	$(0.89 \pm 0.03)^a$	3.8 ± 0.1 $(3.8 \pm 0.5)^b$	3.2 ± 0.2
23			3.1 ± 0.2
46.5			3.1 ± 0.1
70.5			3.1 ± 0.2
154		3.7 ± 0.2	
179	$(0.37 \pm 0.03)^a$		

[a] From ref. 19. [b] From ref. 18.

p-CreOH$(H_2O)^+$ ions formed upon one-colour two-photon ionization 69 600–69 700 cm^{-1}. As can be seen in Fig. 2, the loss of the water molecule is the dominant channel in the D_0 state in the above mentioned energy range.

In order to determine the ionization threshold of the cyclic-OH–OH_2–NH_3 isomer and the threshold for evaporation of solvent molecules, resonant two-colour two-photon ionization experiments were conducted. The pump laser was tuned resonantly to the second transition of the complex (34 815 cm^{-1}) with the laser intensity low enough to preclude one-colour ionization. The ionization laser wavelength was scanned in the range 27 910–30 185 cm^{-1}, while the ions intensities were integrated on the mass channels of *p*-CreOH$(NH_3)^+$, *p*-CreOH$(H_2O)^+$ and *p*-CreOH$(H_2O)(NH_3)^+$. A similar experiment was performed by tuning the pump laser off-resonance of the transition of the cyclic-(OH–OH_2–NH_3) isomer at 34 810 cm^{-1}. In the latter case, the observed signal corresponds to the two-colour two-photon ionization of larger clusters, which show a broad absorption spectrum. The off-resonance signal was subtracted from the signal obtained on-resonance and the ions intensities obtained from the difference are shown in Fig. 3 as a function of the total energy.

Fig. 3 shows that the ionization threshold of the cyclic-(OH–OH_2–NH_3) isomer is located below 62 625 cm^{-1}, which is the lowest energy value accessed with our experimental set-up. A linear extrapolation of the experimental photoionization curve rendered a value of $\sim$62 500 cm^{-1}.

The H_2O evaporation shows a threshold at 62 800 cm^{-1}, as determined from the onset in Fig. 3, and monotonical enhancement of the evaporation rate with total energy. The NH_3 evaporation threshold seems to be also close to that value but with a smaller energy dependence. Since these values correspond to the appearance thresholds, whose determinations are conditioned by the sensitivity of the technique and of the experimental set-up, they should be taken as upper limits to the actual values.

3.b DFT calculations results

3.b.(i) Minimum energy pathway for the isomerization in the S_0 state. As mentioned in the Introduction, two different cyclic isomers can be characterized on the S_0 state PES: the cyclic-(OH–OH_2–NH_3) (Fig. 1a) and the cyclic-(OH–NH_3–OH_2) (Fig. 1b) structures. Considering the near-degeneracy (ΔE = 248 cm^{-1}) of these two structures associated with two different H-bonded networks, *i.e.* OH$\cdots$OH–H$\cdots$$NH_3$ and OH$\cdots$$NH_2$–H$\cdots$$OH_2$, the PES associated with the isomerization between these two structures has been explored.

The energy profile followed by integrating the intrinsic reaction coordinate (IRC) is given in the upper panel of Fig. 4. Structure II shown in Fig. 5 is the optimized transition state (TS) structure which is located 7503 cm^{-1} above the lowest cyclic-(OH–OH_2–NH_3) isomer (structure I, Fig. 5). The analysis of the normal mode associated with the imaginary frequency (i897 cm^{-1}) of the transition state is shown as arrows in structure II. As can be seen in Fig. 4 (upper panel), the energy profile connecting the TS (structure II, Fig. 5) and the cyclic-(OH–NH_3–OH_2) isomer (structure V, Fig. 5) has a shoulder.

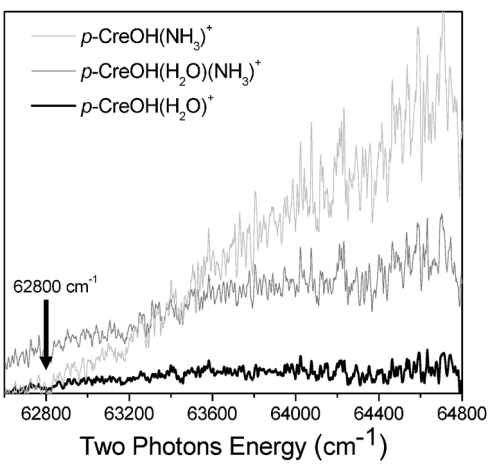

Fig. 3 Photoions yield curves recorded at the masses of (—) [*p*-CreOH$(H_2O)(NH_3)]^+$, (—) [*p*-CreOH$(NH_3)]^+$ and (—) [*p*-CreOH$(H_2O)]^+$. The curves are the result of the difference of the signals recorded with the excitation laser tuned *on* (34 815 cm^{-1}) minus *off* (34 810 cm^{-1}) resonance, depicted in Fig. 2. See the text (Section 3.a.ii) for more details.

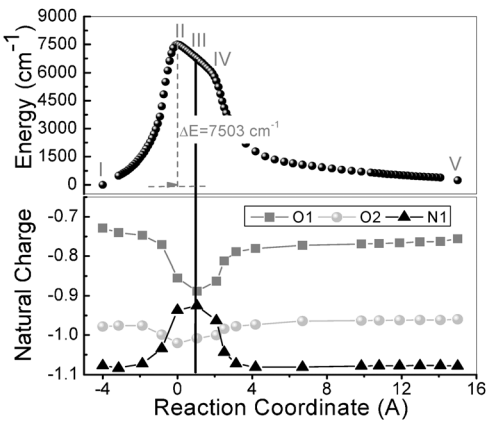

Fig. 4 Energy profile of the IRC for the isomerization from cyclic-(OH–OH_2–NH_3) to cyclic-(OH–NH_3–OH_2), in the S_0 state of the neutral complex (upper panel). Evolution of the natural charge on the heavier (O1, O2 and N1) atoms of the H-bonded network, along the IRC as obtained from the Natural Population Analysis of the electronic wavefunction. The calculations were performed at the DFT-B3LYP/6-311G++(d,p) level of theory.

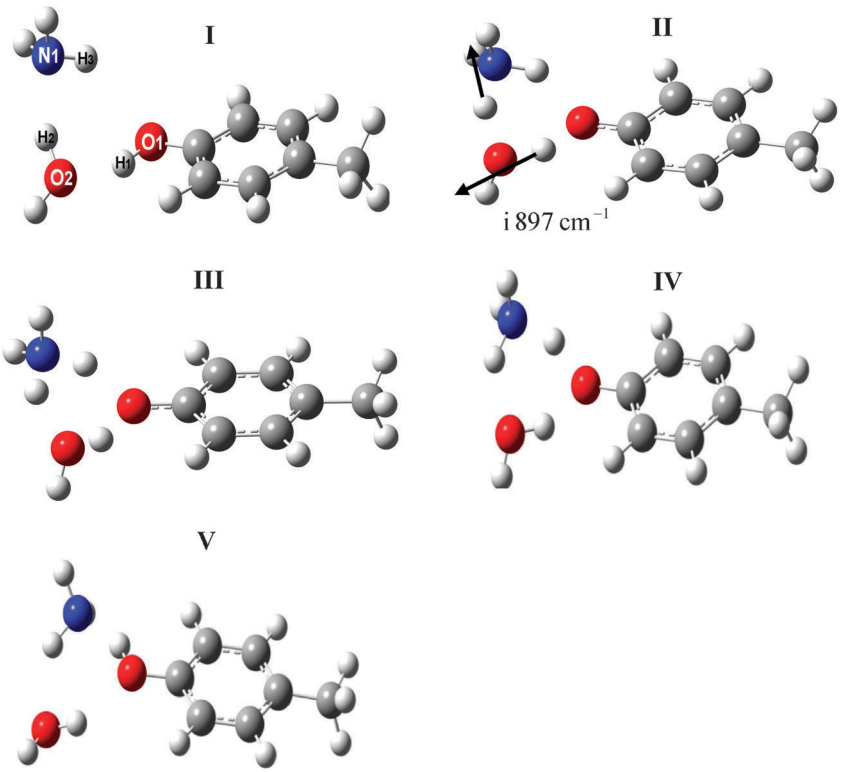

Fig. 5 Most important structures (I–V) along the IRC for the isomerization reaction in the S_0 state shown in the upper panel of Fig. 4. The calculations were performed at the DFT-B3LYP/6-311G++(d,p) level of theory.

This shape of the PES is a typical signature of a strong avoided crossing or, in other words, of a non-monotonic evolution of the electronic structure.[20] This is supported by the Natural Population Analysis (NPA) of the electronic wavefunction. The NPA is illustrated in the lower panel of Fig. 4, where the evolution of the charge on the heavy atoms (O1, O2 and N1) of the H-bonded network along the reaction pathway is depicted. As can be seen in the lower panel of Fig. 4, the charge on the N1 atom reaches a maximum going from the TS (structure II) to the cyclic-(OH–NH_3–OH_2) isomer (structure V). Interestingly, this increase of the nitrogen positive charge is associated with the formation of an NH_4^+ moiety, suggesting the formation of an intermediate ion-pair as illustrated by structure III (Fig. 5) of the cluster in this region of the PES. This ion-pair intermediate will be discussed in Section 4.a. The most relevant bond distances of the structures shown in Fig. 5 are reported in Table S1 (ESI†).

3.b.(ii) Energetics and minimum energy pathway for the isomerization in the D_0 state. To get further insight into the experimental results, the potential energy surface of the ionic D_0 state has been explored, and key stationary points have been characterized. Furthermore, the vertical (IP_v) and adiabatic (IP_{ad}) ionization potentials of both cyclic-(OH–OH_2–NH_3) and cyclic-(OH–NH_3–OH_2) isomers were also calculated. The results are presented in Fig. 6.

The IP_v of the cyclic-(OH–OH_2–NH_3) isomer is 61 903 cm^{-1} while the corresponding value for the cyclic-(OH–NH_3–OH_2) isomers is 62 830 cm^{-1}. Starting from these two neutral cyclic structures, geometry optimizations have been carried out in the ionic D_0 state in order to locate the minima. No cyclic minimum could be found on the ground state ionic PES. All geometry optimizations led to the opening of the intermolecular H-bonded cycles, resulting in chainlike isomers with either the NH_3 or H_2O molecules as terminal moieties. A similar ring opening in the D_0 state was observed in the case of the [*trans*-formamide$(H_2O)_4$]$^+$ complex.[14] In addition, the chain-(OH–NH_3–OH_2)$^+$ isomer is more stable than the chain-(OH–OH_2–NH_3)$^+$ isomer by 1542 cm^{-1} at the B3LYP/6-311G++(d,p) level.

The asymptotic states considering either the evaporation of water or ammonia have been determined. The energy thresholds for three evaporation channels with respect to the cyclic-(OH–OH_2–NH_3) isomer are given in Fig. 6. The states corresponding to the loss of the "terminal" ligand from the two chain-like ionic structures have been characterized. The threshold corresponding to the loss of the terminal NH_3 was found to be 62 609 cm^{-1}, *i.e.* close to the IP_v. The asymptotic state corresponding to the loss of water was found to be lower in energy (60 056 cm^{-1}).

A third asymptotic state, corresponding to an alternative pathway for the loss of a water molecule, has been characterized. This state is obtained by extracting the water molecule from the structure reached by the vertical ionization of the cyclic-(OH–H_2O–NH_3) isomer, hereafter *direct evaporation*. This process renders a water evaporation threshold of 67 180 cm^{-1} and the optimized structure of the [*p*-CreOH(NH_3)]$^+$ product shown in the left-top part of Fig. 6, with the NH_3 molecule as a hydrogen acceptor from the C–H of the *p*-CreOH$^+$ cation, in the *ortho* position and *trans* conformation with respect to the OH group.

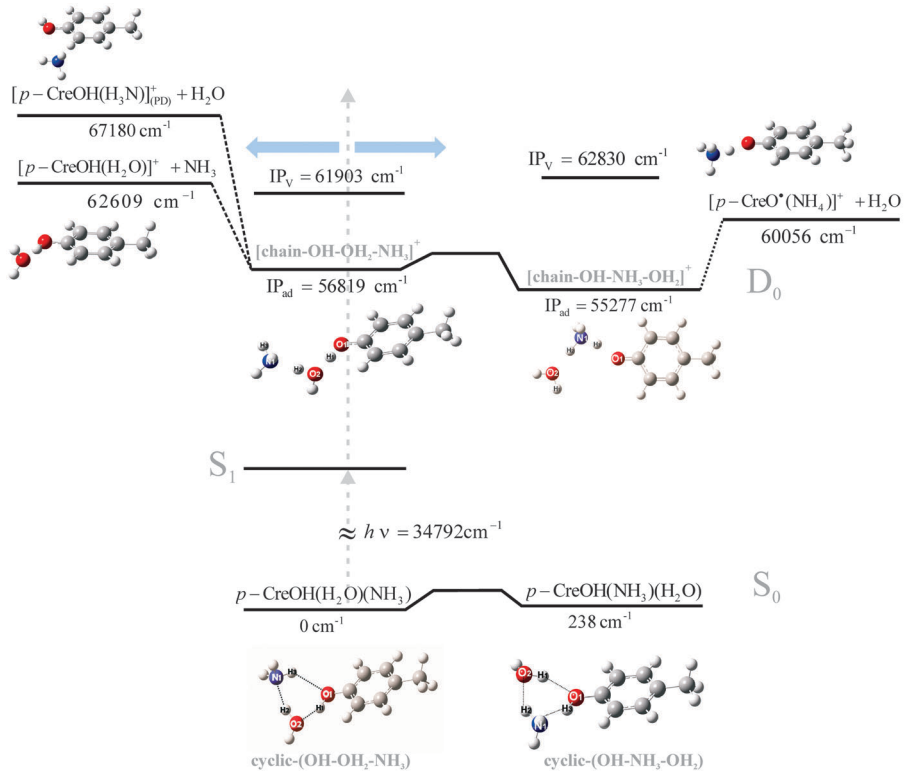

Fig. 6 Schematic energy diagram of the ionization, isomerization and evaporation processes in the D_0 state of the ionic complex, calculated at the DFT-UB3LYP/6-311G++(d,p) level of theory. The $S_1 \leftarrow S_0$ transition energy (34 792 cm^{-1}) is the unique experimental value in this figure. The chain-$(OH–NH_3–OH_2)^+$ isomer is more stable by 1542 cm^{-1} than the chain-$(OH–OH_2–NH_3)^+$ isomer.

The reaction pathway for the isomerization from chain-$(OH–OH_2–NH_3)^+$ to chain-$(OH–NH_3–OH_2)^+$ has also been computed. A single transition state has been characterized and the IRC method has been used to calculate the minimum energy path. Fig. 7a (upper panel) shows the calculated IRC that exhibits an energy barrier of only 575 cm^{-1}. The first point (structure I) in the IRC corresponds to the optimized structure of the chain-$(OH–OH_2–NH_3)^+$ isomer, as shown in Fig. 8. However, the last point calculated for the IRC (structure III) is not a stationary point. As can be seen in Fig. 8, the transition from structure I to structure III is the result of a double proton transfer: from the O1–H1 group of the chromophore to the H_2O molecule, and from the H_2O molecule to the NH_3 molecule. This is also evidenced by the analysis of the normal mode associated with the imaginary frequency (i409 cm^{-1}) of the TS (shown as arrows in structure II). The chain-$(OH–NH_3–OH_2)^+$ isomer (structure VI) could not be reached using the IRC method. In order to

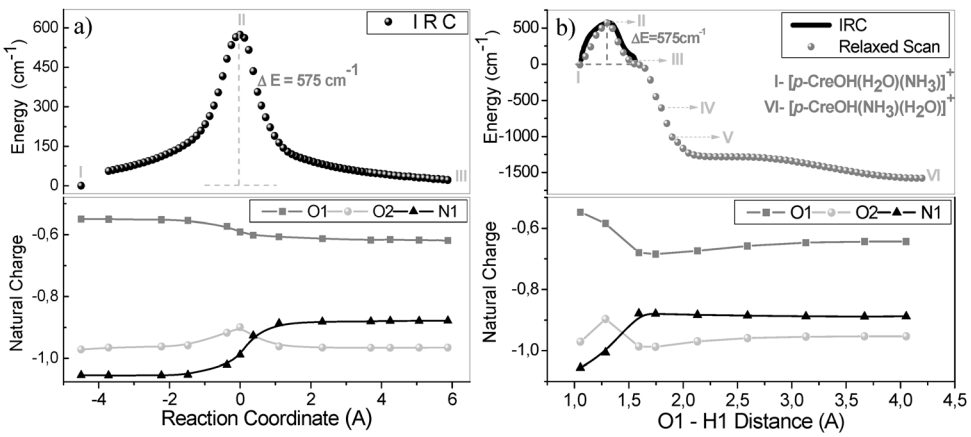

Fig. 7 (a) (upper panel) Energy profile of the IRC in the transition state region of the isomerization from chain-$(OH–OH_2–NH_3)^+$ to chain-$(OH–NH_3–OH_2)^+$, in the D_0 state. (b) (upper panel) (●) Energy profile of the relaxed scan along the O1–H1 distance coordinate built at the 0.05 Å step and (—) energy profile of the IRC calculation as a function of the O1–H1 distance. (lower panel) Evolution of the natural charge on the heavier (O1, O2 and N1) atoms of the H-bonded network, along the IRC (a) and the O1–H1 distance (b) as obtained from the Natural Population Analysis of the electronic wavefunction. The calculations were performed at the DFT-UB3LYP/6-311G++(d,p) level of theory.

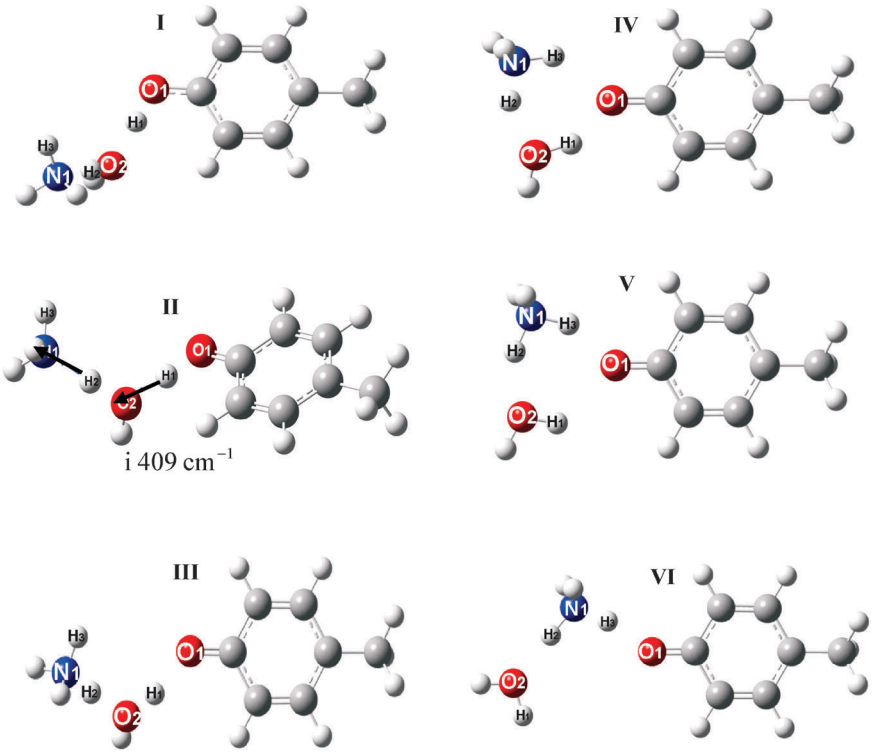

Fig. 8 Most important structures (I–VI) along the isomerization reaction coordinate in the D_0 state shown in the upper panels of Fig. 7. The calculations were performed at the DFT/UB3LYP (6-311G++(d,p)) level of theory.

explore the PES between structure III and the chain-$(OH–NH_3–OH_2)^+$ isomer, a relaxed scan was performed. The lowest energy path was found using the O1–H1 distance as a coordinate for the relaxed scan. The most relevant bond distances of the structures shown in Fig. 8 are reported in Table S2 (ESI†).

The energy profile associated with the interconversion of the two chain-like ionic structures is given in the upper panel of Fig. 7b. The solid line in this figure represents the results of the IRC calculation plotted as a function of the O1–H1 distance. The agreement between both calculations indicates that the O1–H1 distance can be considered as the reaction coordinate. In addition, the same structures I, II and III were obtained irrespective of the method of calculation. Similar relaxed scans, performed by elongating the O2–H2 distance or changing the O1–O2–N1 angle, produce the same energy barrier, structures and energy profiles. It should be noted, however, that these energy profiles are higher in energy than the one obtained by considering the O1–H1 as a reaction coordinate.

In the relaxed scan (Fig. 7b), it is worth noting the presence of two shoulders at 1.75 Å and at 2.75 Å, indicating that the minimum energy pathway involves more than one single step. However, no stationary point other than structures I, II and VI could be characterized along the energy pathway.

In addition to the intermediate geometries connecting both isomers, Fig. 8 shows that structure VI is the same as the optimized structure of the chain-$(OH–NH_3–OH_2)^+$ isomer. The evolution of the charge on the different atoms along the reaction pathway, obtained from the NPA, is depicted in the lower panels of Fig. 7.

4. Discussion

4.a H-bonded network isomerization in the S_0 state

As mentioned above, the S_0 PES associated with the isomerization between the two cyclic H-bonded isomers (Fig. 4, upper panel) has a shoulder which is a clear signature of a strong avoided crossing with an intermediate diabatic electronic state.[20] The analysis of the evolution of the interatomic distances in the structures shown in Fig. 5 and of the atomic (NPA) charges (Fig. 4, lower panel) consistently support the fact that isomerization from the cyclic-$(OH–OH_2–NH_3)$ (structure I) to the cyclic-$(OH–NH_3–OH_2)$ (structure V) proceeds through an ion pair intermediate (p-$CreO^-(H_2O)(NH_4)^+$). For instance, going from the cyclic-$(OH–OH_2–NH_3)$ (structure I) to the TS (structure II), H1 and H2 have been partially displaced toward O2 and N1, respectively, while H3 moved toward O1 but to a lesser extent. This is consistent with the NPA charges (Fig. 4, lower panel), which shows that the natural charge on the O2 atom does not change significantly since it transfers a proton (H2) to the N1 atom while it accepts another proton (H1) from O1. On the other hand, the charge on O1 decreases while on N1 increases due to a partial double proton transfer process from p-CreOH to H_2O and from H_2O to NH_3.

This double proton transfer leads to the formation of the ion pair intermediate (p-$CreO^-(H_2O)(NH_4)^+$) in the region of the shoulder (structure III in Fig. 5). In this structure III, the lengths of the two N–(H2/H3) bonds involved in the proton transfer process are slightly longer (4% and 7%) than in the case of the N–H bond length of the isolated NH_4^+ (1.0265 Å), while the other two N–H bond lengths are 1% shorter. Since the avoided crossing with this ion-pair intermediate

(p-CreO$^-$(H$_2$O)(NH$_4$)$^+$) occurs near the TS, it is likely to be the origin of the lower-energy isomerization barrier.

After the intermediate ion pair (structure III in Fig. 5) is generated, the O1–N1 distance decreases from 2.60 Å to 2.48 Å as a consequence of the electrostatic attraction between the NH_4^+ cation and the p-CreO$^-$ anion. This shortening of the O1–N1 distance triggers a third proton transfer from NH_4^+ to p-CreO$^-$ resulting in the formation of the cyclic-(OH–NH$_3$–OH$_2$). This third proton transfer process is also reflected on the NPA (Fig. 4, lower panel) which shows that beyond the ion pair formation (structure III), the natural charges on O1 and N1 recover their initial values calculated for the cyclic-(OH–OH$_2$–NH$_3$) isomer.

To conclude, the isomerization in the S_0 state proceeds through a triple proton transfer and is assisted by the formation of an intermediate ion pair with an energy barrier large enough (7503 cm^{-1}) to allow the H-bonded network reorganization once the complexes are formed in the supersonic expansion or even at room temperature.

4.b Reactivity and H-bonded network isomerization in the S_1 state

The new determination of the excited state lifetime of the complexes, although different values were obtained, confirms that the value for the cyclic-(OH–OH$_2$–NH$_3$) (Table 1) is closer to that of the p-CreOH(H$_2$O) complex than to that of the p-CreOH(NH$_3$) complex. As mentioned previously,[15] this suggests that the H$_2$O molecule acts as an H-acceptor from the OH group of the chromophore. As a result, it can be considered that the excited state hydrogen transfer (ESHT) reaction channel (eqn (1)) is energetically closed upon excitation to the origin of the electronic transition.[15] Therefore the excited state lifetime is governed by the internal conversion to the S_0 state as in the case of the PhOH(H$_2$O)[2,21–23] and p-CreOH(H$_2$O)[18] complexes.

On the other hand, if the excited state of the cyclic-(OH–NH$_3$–OH$_2$) isomer is accessed either by direct photoexcitation or by isomerization of the locally excited cyclic-(OH–OH$_2$–NH$_3$) isomer, the ESHT from the OH group of the chromophore to the NH$_3$ molecule becomes an energetically open channel[15] and it should be manifested as a shortening on the excited state lifetime of the chromophore within the complex.

Table 1 shows that the excited state lifetime of the cyclic-(OH–OH$_2$–NH$_3$) complex is independent of the internal energy in the S_1 state up to 75 cm^{-1} above the origin. This strongly suggests that neither the ESHT channel nor the isomerization from cyclic-(OH–OH$_2$–NH$_3$) to cyclic-(OH–NH$_3$–OH$_2$) takes place at the excitation energies of this work. This result ensures that the absorption of the second photon to reach the D_0 state of the cation takes place from the excited state of the cyclic-(OH–OH$_2$–NH$_3$) isomer.

It is noteworthy to stress that the lifetimes of PhOH and p-CreOH chromophores do not evolve the same way upon micro-solvation. While the excited state lifetimes of PhOH (2.2 ns)[2,19,22,23] and p-CreOH (1.6 ns)[18,19] are similar, the S_1 lifetimes of the PhOH(H$_2$O) (15 ± 2 ns) and p-CreOH(H$_2$O) (3.8 ± 0.5 ns) complexes are very different. While no explanation can be provided, it is interesting to observe that the effect of the substitution by a CH$_3$ group is more important in the complex with H$_2$O than in the complex with NH$_3$, for which the S_1 lifetime is twice shorter than the S_1 lifetime of the bare molecules in both PhOH and p-CreOH.[19]

In addition, following the electronic spectral shift rule,[1] a red-shift in an electronic transition due to the intermolecular hydrogen bonding indicates that the H-bond in the corresponding electronically excited state is strengthened as compared to the same property in the ground electronic state, because of the charge redistribution. In this case, the experimental results show a red-shift of 539 cm^{-1}, which means that the H-bond strength increases by ~6.5 kJ mol^{-1} upon electronic excitation. In the case of the p-CreOH(NH$_3$) complex the electronic red-shift is 637 cm^{-1} (7.6 kJ mol^{-1})[16] while for the p-CreOH(H$_2$O)[18] complex the electronic red-shift is 351 cm^{-1} (4.2 kJ mol^{-1}). These results show a cooperative effect between the H-bonds of H$_2$O and NH$_3$, in the mixed complex. The OH···OH$_2$ bond is strengthened not only by the electronic excitation but also by the presence of a new H-bond (OH$_2$···NH$_3$) that increases the hydrogen/proton affinity of the water molecule.

4.c Solvent evaporation and H-bonded network isomerization in the D_0 state

The experimental ionization threshold for the cyclic-(OH–OH$_2$–NH$_3$) complex was estimated to be ~62 500 cm^{-1}. The fact that the experimental value is closer to the calculated IP$_v$ (61 903 cm^{-1}) than to the calculated IP$_{ad}$ (56 819 cm^{-1}) is a typical signature of the different equilibrium geometries in the neutral and ionic states (cyclic- and chain-like structures, respectively) that renders low Franck–Condon (FC) factors for both structures, making difficult the experimental determination of the IP$_{ad}$.

This low FC factor is due to the opening of the H-bonded ring network. This is essentially because the p-CreOH$^+$ radical cation is a distonic ion formed as a result of an electron transfer from the hydroxyl group to the π aromatic system. A similar electron transfer is expected in the p-CreOH(H$_2$O)(NH$_3$) cluster. This is evidenced by the comparison of the neutral and cationic structures and atomic charges (NPA). Upon ionization, there is a substantial shortening of the CO bond length (from 1.372 Å to 1.314 Å at the level of theory of this work). Also, the NPAs (Fig. 4 and 7, lower panels) show that the natural charge on the O1 atom of p-CreOH in the S_0 state of the cyclic-(OH–OH$_2$–NH$_3$) isomer is −0.74 but it becomes −0.55 in the D_0 optimized structure, thus reducing the attractive force between the NH$_3$ molecule and the OH group. This fact, in addition to the repulsive force between the partially positively-charged H3 atom of the NH$_3$ molecule and the positively charged p-CreOH$^+$ cation triggers the opening of the H-bonded cyclic structure. A similar explanation was recently suggested to account for the water migration in *tert*-acetanilide(H$_2$O) complex upon photoionization.[11]

It is thus clear that under the present experimental conditions, only the ionization of the neutral cyclic-(OH–OH$_2$–NH$_3$) isomer is observed. The energy threshold for the evaporation of either H$_2$O or NH$_3$ was estimated to be 62 800 cm^{-1}. The value is very close to the calculated value (62 609 cm^{-1}) for the evaporation of NH$_3$. As discussed above, the H-bonded ring network of the cyclic-(OH–OH$_2$–NH$_3$) neutral isomer opens upon ionization. As a result, the NH$_3$ evaporation should correspond to a simple bond cleavage from the resulting ionic

chain-$(OH–OH_2–NH_3)^+$ structure. Nevertheless, this *direct* evaporation process of NH_3 is a minor process since a selective water evaporation is observed experimentally. Based on our investigation of the ionic PES, the only energetic accessible water evaporation asymptote (predicted at 60 056 cm^{-1}) corresponds to an *isomerization-assisted* process proceeding through a solvent rearrangement.

Since the internal energy in the ion is large, as well as the states density, the different yields of both evaporation channels can be ascribed, from a statistical point of view, to the lower energy necessary to evaporate a H_2O molecule as compared to that for NH_3 evaporation. As a result, the energy dependence of the ratio of both evaporation channels is well reproduced using a simple Rice–Ramsperger–Kassel–Marcus (RRKM) calculation.

Although, statistical energy distribution is likely to be at the origin of the preferential evaporation of H_2O, which corresponds to the lowest energy evaporation channel, this process requires isomerization of the whole H-bonded network that proceeds through a tight transition state. Thus, the dynamics of the isomerization processes deserves a particular attention. Fig. 7 shows the minimum energy pathway calculated for the isomerization process that precedes the H_2O evaporation. The isomerization process is energetically allowed since the energy barrier for the isomerization from chain-$(OH–OH_2–NH_3)^+$ to chain-$(OH–NH_3–OH_2)^+$ is 575 cm^{-1} while the excess energy of the cation upon vertical ionization is 5000 cm^{-1}. Nevertheless, since the isomerization takes place through the rearrangement of all the nuclei of the H-bonded network, in order to be competitive with the energy allowed *direct evaporation* of NH_3, it is likely that the isomerization is favoured by the excited vibrational state initially populated upon vertical ionization of the neutral cyclic-$(OH–OH_2–NH_3)$ isomer.

In order to evaluate which excited vibrational states are initially populated, two geometrical indices are defined based on the differences between the cyclic-$(OH–OH_2–NH_3)^+$ geometry reached upon vertical photoionization and the equilibrium geometry of the chain-$(OH–OH_2–NH_3)^+$ ionic complex. For each $X–Y$ bond length, a $\%RCr^{X-Y}$ (eqn (1)) index can be defined.

$$\%RCr^{X-Y} = \frac{r^{X-Y}_{\text{vertical}} - r^{X-Y}_{\text{equilibrium}}}{r^{X-Y}_{\text{equilibrium}}} \times 100 \qquad (1)$$

Depending on whether the $X–Y$ bond distance decreases or increases from the cyclic- to the chain-like structure, this $\%RCr^{X-Y}$ bond index is positive or negative, respectively. Similarly, for each $X–Y–Z$ bond angle, a $\%RC\alpha^{X-Y-Z}$ (eqn (2)) index is also defined.

$$\%RC\alpha^{X-Y-Z} = \frac{\alpha^{X-Y-Z}_{\text{vertical}} - \alpha^{X-Y-Z}_{\text{equilibrium}}}{\alpha^{X-Y-Z}_{\text{equilibrium}}} \times 100 \qquad (2)$$

Only values of the two indices larger than 2% are given in Fig. 9. The bond distances and angles involving the aromatic ring and the CH_3 group do not change significantly while the major variations are observed in the H-bonded network. Then, upon vertical ionization the nuclei of the atoms involved in this H-bonded network will undergo rearrangement to reach the equilibrium geometry and therefore vibrational

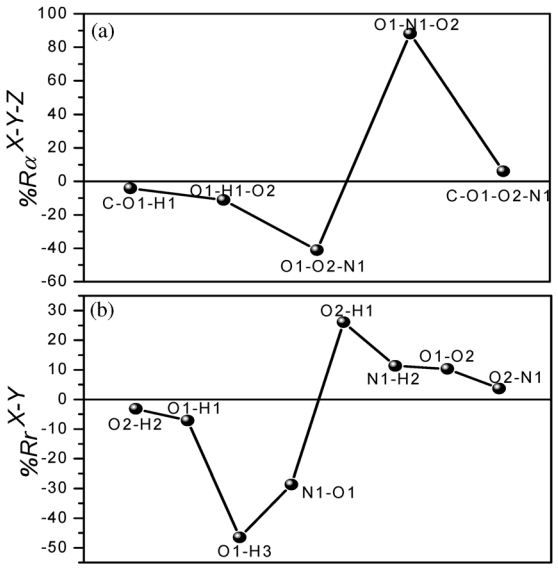

Fig. 9 Geometrical indices for the bond (a) angles ($\%RC\alpha^{X-Y-Z}$) and (b) distances ($\%RCr^{X-Y}$) that quantify the differences between the cyclic-$(OH–OH_2–NH_3)^+$ geometry reached upon vertical photoionization and the equilibrium geometry of the chain-$(OH–OH_2–NH_3)^+$ ionic complex, calculated according to eqn (1) and (2). Positive or negative $\%RCr^{X-Y}$ or $\%RC\alpha^{X-Y-Z}$ values indicate that the particular bond distance or angle in the vertical structure is larger or smaller than in the equilibrium geometry, respectively.

excitation is expected in the modes involving the H-bonded (O1–H1–O2–H2–N1–H3) atoms.

Fig. 9 shows that the O1–H1 and O2–H2 distances in the vertical structure are shorter than in the equilibrium geometry while the distances O2–H1 and N1–H2 are longer. Consequently, vibrational excitation is expected in the modes involving the O1–H1, O2–H2, O2–H1 and N1–H2 stretches. In addition, the observation that $\%RC\alpha^{O1-N1-O2} = 88\%$ and $\%RC\alpha^{O1-O2-N1} = -41\%$ indicates that vibrational excitation is also expected in the modes involving these angles.

Interestingly, the analysis of the normal mode associated with the imaginary frequency (i409 cm^{-1}), depicted in structure II of Fig. 8, shows that this mode involves the elongation of the O1–H1 and O2–H2 bonds and the shortening of the O2–H1 and N1–H2 bonds.

The reaction coordinate also has a large component on the O1–N1–O2 and O1–O2–N1 angles (Fig. 8), which is in agreement with the fact that the two bond angle indices of these modes are large. Beyond the TS the NPA (Fig. 7, lower panel) shows that a double proton transfer takes place and the chemical structure of the complex is chain-$(O–OH_2–NH_4)^+$. This fact, in addition to the large vibrational excitation on the O1–N1–O2 and O1–O2–N1 angles that promotes the oscillation of the $O–OH_2–NH_4^+$ chain, allows the interaction between the NH_4^+ moiety and O1 atom, that results in the formation of the most stable chain-$(OH–NH_3–OH_2)^+$ isomer (structure VI in Fig. 8).

This analysis of the geometrical indices clearly shows that the excited vibrational energy deposited through the vertical ionization of the cyclic-$(OH–OH_2–NH_3)$ structure is essentially deposited in the reaction coordinate associated with the isomerization of the ionic cluster towards the chain-$(OH–NH_3–OH_2)^+$ structure, which will then easily evaporate H_2O.

The analysis of the geometrical parameters of the structure of the final product $[p\text{-CreOH}(NH_3)]^+$ of the H_2O evaporation process reveals a proton transfer from $p\text{-CreOH}^+$ to NH_3. For instance, the N–H^+ distance is 1.107 Å and the O–H^+ distance is 1.271 Å. As a result, the ion formed in the lowest fragmentation energy channel can be considered as a distonic ion complex formed between the *p*-CreO radical and the NH_4^+ cation.

The experimental value of the proton affinity (PA) of the *p*-CreO radical is 884.5 kJ mol^{-1}, only slightly larger than the PA of NH_3 (853.6 kJ mol^{-1}) which is significantly larger than the one of water (691 kJ mol^{-1}). In this respect, it is worth noting that the relative orders of the PA's of these three systems are well reproduced at the level of theory of this work (*p*-CreO: 882.9; NH_3: 845.7; H_2O: 691.0 kJ mol^{-1}). The formation of an NH_4^+ as a product or an intermediate along the rearrangement coordinate within the ionic, or even more in the neutral cluster, might be surprising. However, it is important to stress that when the PA's of two basic molecules (B and B′) are within 25–50 kJ mol^{-1}, the potential energy surface along the proton asymmetric stretch is extremely flat.[24] Furthermore, it should be noted that the structure of two monomers bound by a proton is not only driven by the difference of PAs, as shown recently by Fridgen *et al.* The electrostatic interactions between the protonated monomer and the other might play a significant role, especially when the latter carries a large dipole moment.[25,26]

Finally, it should be also noticed that the calculated value of the PA of the $(H_2O)(NH_3)$ cluster is 909.3 kJ mol^{-1}, *i.e.* larger than the calculated value of the *p*-CreO radical. This PAs difference is the driving force for the initial proton transfer from $p\text{-CreOH}^+$ to $(H_2O)(NH_3)$.

5. Conclusions and implications

The H-bonded network rearrangement in the S_0, S_1 and D_0 states of the neutral and cationic $p\text{-CreOH}(H_2O)(NH_3)$ complexes was studied experimentally and theoretically and a comparison of this process in the three states is given.

5.a Rearrangement in the S_0 state

The isomerization from the cyclic-(OH–OH_2–NH_3) to the quasi-isoenergetic cyclic-(OH–NH_3–OH_2) isomer proceeds through a non-concerted triple proton transfer mechanism. The analysis of the evolution of the atomic charges, and also of the geometrical parameters, clearly shows that a shoulder on the energy profile connecting the two cyclic isomers corresponds to the formation of an intermediate ion pair $p\text{-CreO}^-(H_2O\text{–}NH_4^+)$. The energy barrier, however, is too high (7503 cm^{-1}) to be overcome at the temperature of the supersonic expansion.

5.b Rearrangement in the S_1 state

The excited state lifetimes of the $p\text{-CreOH}(H_2O)(NH_3)$ and $p\text{-CreOH}(H_2O)$ complexes were re-determined. The experimental results show that the S_1 state lifetime of the $p\text{-CreOH}(H_2O)(NH_3)$ complex is closer to the S_1 state lifetime of the $p\text{-CreOH}(H_2O)$ complex than to the S_1 lifetime of the $p\text{-CreOH}(NH_3)$ complex. This fact re-confirms that the H_2O molecule acts as an H-acceptor of the OH group of the chromophore molecule (cyclic-(OH–OH_2–NH_3) isomer). In addition, the S_1 state lifetime of the cyclic-(OH–OH_2–NH_3) isomer is independent of the excitation energy within 75 cm^{-1} above the origin of the electronic transition. This is evidence that neither the ESHT channel nor the isomerization from cyclic-(OH–OH_2–NH_3) to cyclic-(OH–NH_3–OH_2) takes place at the excitation energies of this work and ensures that the absorption of the second photon to reach the D_0 state takes place from the S_1 state of the cyclic-(OH–OH_2–NH_3) isomer.

5.c Rearrangement in the D_0 state

The preferential evaporation of H_2O was observed upon vertical ionization of the cyclic-(OH–OH_2–NH_3) isomer and it was suggested that a statistical behaviour is likely to be at the origin of this result. It was shown that, a fast rearrangement of the H-bonded network is required for the evaporation of H_2O in the ion. The reaction pathway for the solvent rearrangement involves a double proton transfer process with a very low energy barrier (575 cm^{-1}) that is overcome at the vertical ionization energy of the complex. As compared to a direct NH_3 loss, *i.e.* a simple bond cleavage, the H_2O evaporation process, which corresponds to the lowest energy evaporation channel, is likely to be entropically disfavoured since it proceeds through a tight transition state. It is thus important to stress that the analysis of differential geometry between the vertically ionized cyclic-$(OH\text{–}OH_2\text{–}NH_3)^+$ and the equilibrium chain-$(OH\text{–}OH_2\text{–}NH_3)^+$ isomers suggests that the vibrational modes associated with the isomerization are highly excited. The selectivity of the H_2O loss may thus also be in part due to the dynamics of the rearrangement which is facilitated by the initial excited vibrational state.

To the best of our knowledge, it is the first time that the exchange of H-acceptor and H-donor solvent molecules in the same functional group is reported. In the light of the present results and those reported by several groups during the last few years, gas phase clusters appear as interesting models for understanding the dynamics of H-bonded network rearrangement in molecular complexes.

In the present study, the S_1 state dynamics of the $p\text{-CreOH}(H_2O)(NH_3)$ complex is dominated by the structure of the H-bonded network, in which the H_2O molecule acts as an H-acceptor of the OH of the chromophore, rendering a long lived excited state because the ESHT channel is energetically closed. However, upon ionization of the complex the spectrum and dynamics are observed mainly on the mass of the smaller $p\text{-CreOH}(NH_3)^+$ complex without H_2O, due to the preferential *isomerization assisted* water evaporation in the ion.

An important conclusion of this work is that when studying excited state dynamics of neutral complexes using ionization probes, one should carefully consider the potential dynamics within the ionized state. This is especially true considering that water is a common impurity in the compounds used to study hydrogen or proton transfer reactions. In the present case, for instance, the spectrum and excited state dynamics of water contaminated chromophore$(OH_2)(NH_3)_n$ complexes could be observed on the masses of the smaller chromophore$(NH_3)_n^+$ complexes. In order to prevent erroneous interpretations, the possible isomerization and evaporation processes in the ion must be considered when studying the excited state dynamics of such complexes.

Acknowledgements

This work was supported by MinCyT-Córdoba, ANPCyT, SeCyT-UNC, CONICET and the CNRS/CONICET exchange program.

References

1 G.-J. Zhao and K.-L. Han, *Acc. Chem. Res.*, 2011, DOI: 10.1021/ar200135h, and references therein.
2 G. A. Pino, *Recent Advances in Nanoscience*, Research Signpost, Kerala, 2007, ch. 5.
3 H. Nakagawa and M. Kataoka, *J. Phys. Soc. Jpn.*, 2010, **79**, 08380, and references therein.
4 T. S. Zwier, *Annu. Rev. Phys. Chem.*, 1996, **47**, 205.
5 T. Ebata, A. Fujii and N. Mikami, *Int. Rev. Phys. Chem.*, 1998, **17**, 331.
6 B. Brutschy, *Chem. Rev.*, 2000, **100**, 389.
7 H. Sekiya and K. Sakota, *J. Photochem. Photobiol., C*, 2008, **9**, 81.
8 Y. Matsuda, N. Mikami and A. Fujii, *Phys. Chem. Chem. Phys.*, 2009, **11**, 1279.
9 G. A. Pino, I. Alata, C. Dedonder, C. Jouvet, K. Sakota and H. Sekiya, *Phys. Chem. Chem. Phys.*, 2011, **13**, 6325.
10 J. R. Clarkson, E. Baquero, V. A. Shubert, E. M. Myshakin, K. D. Hordan and T. S. Zwier, *Science*, 2005, **307**, 1443.
11 K. Sakota, S. Harada, Y. Shimazaki and H. Sekiya, *J. Phys. Chem. A*, 2011, **115**, 626.
12 H. M. Kim, K. Y. Han, J. Park, G.-S. Kim and S. K. Kim, *J. Chem. Phys.*, 2008, **128**, 041104.
13 M. Gerhards, A. Jansen, C. Unterber and A. Gerlach, *J. Chem. Phys.*, 2005, **123**, 074320.
14 K. Sakota, Y. Shimazaki and H. Sekiya, *Phys. Chem. Chem. Phys.*, 2011, **13**, 6411.
15 A. N. Oldani, J. C. Ferrero and G. A. Pino, *Phys. Chem. Chem. Phys.*, 2009, **11**, 10409.
16 A. N. Oldani, M. Mobbili, E. Marceca, J. C. Ferrero and G. A. Pino, *Chem. Phys. Lett.*, 2009, **471**, 41.
17 M. J. Frisch, G. W. Trucks, H. B. Schlegel, G. E. Scuseria, M. A. Robb, J. R. Cheeseman, J. A. Montgomery, Jr, T. Vreven, K. N. Kudin, J. C. Burant, J. M. Millam, S. S. Iyengar, J. Tomasi, V. Barone, B. Mennucci, M. Cossi, G. Scalmani, N. Rega, G. A. Petersson, H. Nakatsuji, M. Hada, M. Ehara, K. Toyota, R. Fukuda, J. Hasegawa, M. Ishida, T. Nakajima, Y. Honda, O. Kitao, H. Nakai, M. Klene, X. Li, J. E. Knox, H. P. Hratchian, J. B. Cross, C. Adamo, J. Jaramillo, R. Gomperts, R. E. Stratmann, O. Yazyev, A. J. Austin, R. Cammi, C. Pomelli, J. W. Ochterski, P. Y. Ayala, K. Morokuma, G. A. Voth, P. Salvador, J. J. Dannenberg, V. G. Zakrzewski, S. Dapprich, A. D. Daniels, M. C. Strain, O. Farkas, D. K. Malick, A. D. Rabuck, K. Raghavachari, J. B. Foresman, J. V. Ortiz, Q. Cui, A. G. Baboul, S. Clifford, J. Cioslowski, B. B. Stefanov, G. Liu, A. Liashenko, P. Piskorz, I. Komaromi, R. L. Martin, D. J. Fox, T. Keith, M. A. Al-Laham, C. Y. Peng, A. Nanayakkara, M. Challacombe, P. M. W. Gill, B. Johnson, W. Chen, M. W. Wong, C. Gonzalez and J. A. Pople, *GAUSSIAN 03 (Revision–E.01–SMP)*, Gaussian Inc., Pittsburgh, PA, 2003.
18 G. Myszkiewicz, L. Meerts, Ch. Ratzer and M. Schmitt, *J. Chem. Phys.*, 2005, **123**, 044304.
19 G. A. Pino, A. N. Oldani, E. Marceca, M. Fujii, S.-I. Ishiuchi, M. Miyazaki, M. Broquier, C. Dedonder and C. Jouvet, *J. Chem. Phys.*, 2010, **133**, 124313.
20 S. Shaik and A. Shurki, *Angew. Chem., Int. Ed.*, 1999, **38**, 586.
21 A. L. Sobolewski and W. Domcke, *J. Phys. Chem. A*, 2001, **105**, 9275.
22 A. Sur and P. M. Johnson, *J. Chem. Phys.*, 1986, **84**, 1206.
23 R. J. Lipert and S. D. Colson, *J. Phys. Chem.*, 1989, **93**, 135.
24 J. R. Roscioli, L. R. McCunn and M. A. Johnson, *Science*, 2007, **316**, 249.
25 T. D. Fridgen, *J. Phys. Chem. A*, 2006, **110**, 6122.
26 M. B. Burt and T. D. Fridgen, *J. Phys. Chem. A*, 2007, **111**, 10738.